

**Total reaction cross section for the  ${}^6\text{He} + {}^9\text{Be}$  system**K. C. C. Pires,<sup>1</sup> R. Lichtenthaler,<sup>1</sup> A. Lepine-Szily,<sup>1</sup> and V. Morcelle<sup>2</sup><sup>1</sup>*Instituto de Fısica, Universidade de Sao Paulo, C.P. 66318, 05314-970, Sao Paulo, Brazil*<sup>2</sup>*Departamento de Fısica, Universidade Federal Rural do Rio de Janeiro, 23851-970, Seropedica, RJ, Brazil*

(Received 26 May 2014; published 29 August 2014)

Elastic angular distributions of the  ${}^6\text{He} + {}^9\text{Be}$  scattering at  $E_{\text{lab}}=16.2$  and  $21.3$  MeV have been analyzed in the context of the optical model. The projectile-target optical potential was calculated in a cluster model where the contributions from the fragment target ( $\alpha-{}^9\text{Be}$ ) and the dineutron target ( $2n-{}^9\text{Be}$ ) are separated and the latter was searched to reproduce the experimental data. The total reaction cross sections for the  ${}^6\text{He} + {}^9\text{Be}$  system have been obtained, and the error bars have been estimated considering the spread between the present optical model and previous coupled channels and continuum discretized coupled-channels calculations. The cross sections have been reduced and compared in a systematics involving tightly bound, weakly bound, and the exotic  ${}^6\text{He}$  projectiles, all on  ${}^9\text{Be}$  target. An analysis of the enhancements observed in the total reaction cross section induced by  ${}^6\text{He}$  on light, medium mass, and heavy targets is presented.

DOI: [10.1103/PhysRevC.90.027605](https://doi.org/10.1103/PhysRevC.90.027605)

PACS number(s): 25.60.Dz, 21.10.Gv, 24.10.Ht, 24.10.Eq

Low-energy reactions induced by exotic neutron halo projectiles such as  ${}^6\text{He}$  have been investigated over the last years [1–7]. Elastic scattering measurements indicate that the total reaction cross section of neutron halo projectiles such as  ${}^6\text{He}$  [5,7,9],  ${}^{11}\text{Li}$  [8], and  ${}^{11}\text{Be}$  [6] on heavy and medium mass targets is considerably higher than the cross sections of stable projectiles on similar mass targets. Among the nuclei investigated, three classes can be distinguished: the tightly bound nuclei, which are normally double magic such as  ${}^4\text{He}$  and  ${}^{16}\text{O}$ , present the lowest cross sections. The weakly bound projectiles such as  ${}^{6,7}\text{Li}$  and  ${}^9\text{Be}$  present total cross sections higher than the tightly bound but lower than the exotic ones. Finally, the exotic  ${}^6\text{He}$  which presents the higher reaction cross section. The reason for that enhancement lies in part, in the fact that light exotic nuclei normally have a pronounced cluster configuration and are weakly bound, in comparison to their stable isobars. The  ${}^6\text{He}$  nucleus, for instance, has a separation energy of 0.973 MeV to break up into an alpha particle and two neutrons, whereas  ${}^6\text{Li}$  has a separation energy of 1.47 MeV to break into an alpha particle and a deuteron. Tightly bound nuclei such as  ${}^4\text{He}$  and  ${}^{16}\text{O}$ , on the other hand, have a much higher breakup energy, ranging from 7 up to more than 20 MeV. That low breakup threshold make reactions, such as projectile breakup, easy to occur even at low energies. In addition, some neutron-rich exotic nuclei such as  ${}^6\text{He}$  present a halo formed by loosely bound neutrons, which extends to large distances from the core. These nuclei present a large dipole polarizability, making them easy to break up even in the Coulomb field of the target (Coulomb breakup). The effect of the breakup in the Coulomb field is primarily to remove flux from the elastic scattering in the forward angles region, around the position of the Fresnel peak, enhancing the total reaction cross section. This effect is important in the collision involving heavy targets, because of the dependence of the Coulomb breakup form factor with the target atomic number [10,11]. Then a question arises of what happens in collision between the  ${}^6\text{He}$  projectile and light targets, where the Coulomb breakup becomes less and less important and even negligible [10,12]. There are indications that the enhancements observed in the

${}^6\text{He}$  total reaction cross section, with respect to its weakly bound partners  ${}^{6,7}\text{Li}$ , would be very much reduced or even disappear in the case of lighter targets such as  ${}^{27}\text{Al}$  target [3]. More recently a systematic analysis of several systems indicate that the enhancement for  ${}^6\text{He} + {}^{12}\text{C}$  is reduced with respect to the heavy targets [13,14].

Here we present results for the  ${}^9\text{Be}$  target that complement a recent work [15], where  ${}^6\text{He} + {}^9\text{Be}$  elastic angular distributions have been measured at two energies. In Ref. [15] the angular distributions have been analyzed by two approaches: coupled channels (CC), considering the coupling with excited states of the target, and three-body and four-body continuum-discretized coupled-channels (CDCC) calculations, which describe the effect of the coupling between the elastic scattering and the projectile breakup channel. The basic ingredients of the CDCC calculations are the optical potentials which are used to describe the  $\alpha-{}^9\text{Be}$  and  $n-{}^9\text{Be}$  scattering. Those potentials have been obtained from the literature at the relevant energies and consequently, no adjustment of parameters was performed. In this sense, the CDCC calculations presented in Ref. [15] can be considered as predictions for the elastic cross sections. However, this approach does not give a complete description of the  ${}^6\text{He} + {}^9\text{Be}$  scattering. The  ${}^9\text{Be}$  target is also a weakly bound nucleus, with no bound excited states, and can easily break up in the collision. In addition, one and two neutron transfer processes between the projectile and target are expected to play some role in the reaction mechanism [16]. Although the target breakup is somehow taken into consideration in the  $\alpha-{}^9\text{Be}$  optical potential used in the CDCC calculations, we do not expect the CDCC to reproduce all features of the data. In fact, the theoretical results (3b- and 4b-CDCC) presented in Ref. [15] are in fair agreement with the data but, at the higher energy, the agreement is not so good, mainly of the 4b-CDCC at backward angles. This may cast some doubts on the reaction cross sections obtained from these CDCC and CC calculations.

As a complete calculation, including the projectile and target breakup, is beyond our present possibilities, we propose here a different approach.

TABLE I. Parameters of the optical model calculations. The calculation was performed with the folded potential [Eq. (1)] using the parameters given below.

$E_{\text{lab}}$	Potential	$V_0$ (MeV)	$r_0$ (fm)	$a_0$ (fm)	$W_0$ (MeV)	$r_i$ (fm)	$a_i$ (fm)	$\sigma_{\text{reac}}$ (mb)	Ref.
	$\alpha + {}^9\text{Be}$	50.00	1.85	0.55	2.50	1.85	0.55	—	[19]
	$2n + \alpha$	96.06	1.90	0.25	—	—	—	—	[17]
16.2	$2n + {}^9\text{Be}$	61.01	1.51	0.55	20.00	1.20	1.01	1513	—
21.3	$2n + {}^9\text{Be}$	21.41	1.51	0.54	10.02	1.35	1.56	1944	—

The idea is to obtain the best fit of the data, by adjusting the parameters of an optical potential and then to look at the reaction cross sections that come out. For optical potential, however, we use the diagonal part of the CDCC cluster model for the ground state which is given below:

$$V_{\text{opt}} = \langle \phi_{\text{He}}^{(gs)} | V_{[2n+{}^9\text{Be}]} + V_{[\alpha+{}^9\text{Be}]} | \phi_{\text{He}}^{(gs)} \rangle. \quad (1)$$

In this approach, the interaction between the projectile  ${}^6\text{He}$  and the target  ${}^9\text{Be}$  is separated into two contributions, one for the fragment target ( $\alpha$ - ${}^9\text{Be}$ ) which is known and another for the dineutron target ( $2n$ - ${}^9\text{Be}$ ) which is unknown. For the  $\alpha$ - ${}^9\text{Be}$  system, we fixed a Wood-Saxon potential, obtained empirically from experimental data (see Table I). The ( $2n$ - ${}^9\text{Be}$ ) component of the interaction, however, is unknown, because there are no data for the di-neutron scattering. This component, we parametrized by a Wood-Saxon shape, whose six parameters have been freely varied to fit the data. As far as we know this approach is new in pure optical model

applications and was used only in CDCC calculations where no parameter adjustment is made.

The intrinsic projectile wave function ( $\phi_{\text{He}}^{(gs)}$ ) was calculated in the single-particle model, considering the two neutrons as a single particle, bound to the  $\alpha$  core with a separation energy of 1.6 MeV instead of the correct value 0.973 MeV. This modified binding energy was first proposed by Moro in Ref. [17], as a way to reproduce the exact three-body wave function of the  ${}^6\text{He}$ , and was adopted previously in several applications of the CDCC model giving results close to the full four-body model [1,2,15].

All the calculations have been performed using the computer code SFRESCO, part of the code FRESCO [18]. The results are shown in Fig. 1 by the solid line and the resulting parameters for the ( $2n$ - ${}^9\text{Be}$ ) potential are shown in Table I. The optical model calculations reproduce quite well the overall shape of the angular distributions. The oscillations have been smoothed out considering the effect of the experimental angular resolution, as explained in detail in Ref. [15]. The calculation without the convolution with the experimental angular resolution is represented by the dotted line. Some ambiguity was observed between the parameters  $V_0$  and  $r_0$  of the ( $2n$ - ${}^9\text{Be}$ ) potential presented in Table I. Equally good fits can be obtained by increasing  $V_0$  and decreasing  $r_0$ . However, the total reaction cross sections, which are the main goal of the present analysis, are very similar. We chose the solution presented in Table I which preserves a similar geometry ( $r_0$  and  $a_0$ ) for the two energies. The error bars of the OM parameters that come out from the SFRESCO calculations are very small—about 2% for  $r$ , and less than 1% for  $V_0$  and  $W_0$ .

The total reaction cross sections obtained are presented in Table II, together with the results from the CC and CDCC calculations [15]. The CC and 3b-CDCC calculations overestimate the elastic scattering cross sections in the forward angle region, resulting in lower total reaction cross sections, when compared to the present OM calculation.

To compare different systems, the total reaction cross sections obtained from the present OM, and previous CC,

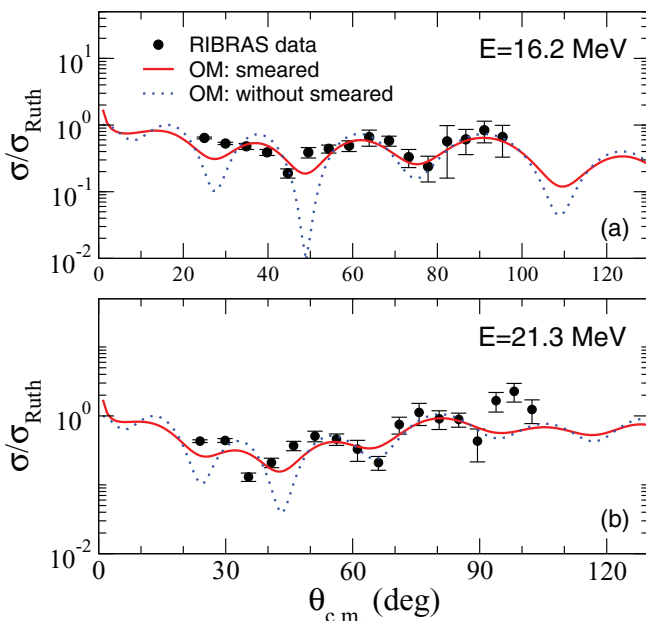


FIG. 1. (Color online) Elastic scattering angular distributions for  ${}^6\text{He} + {}^9\text{Be}$  at (a)  $E_{\text{lab}} = 16.2$  MeV and (b)  $E_{\text{lab}} = 21.3$  MeV. The solid circles are the data and the solid lines are the results of the optical model calculations using the folded potential shown in Table I. These calculations have been convoluted with the experimental resolution [15] and for comparison we also present the calculation without convolution (dotted line).

TABLE II. Total reaction cross sections in mb for OM, CC and CDCC calculations.

$E_{\text{lab}}$	OM	CC	3b-CDCC	4b-CDCC
16.2	1513	1445	1488	1643
21.3	1944	1449	1483	1648

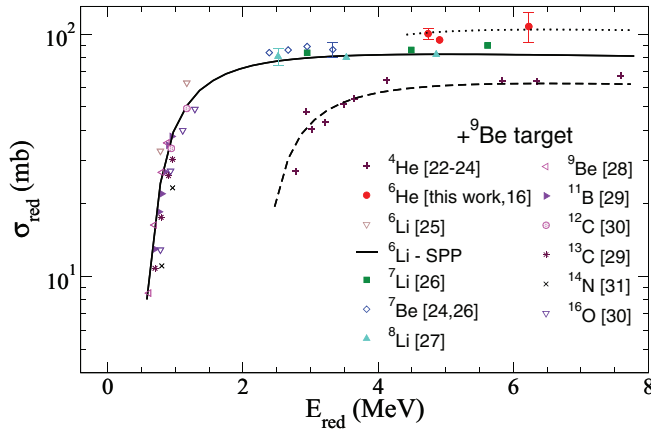


FIG. 2. (Color online) Reduced total reaction cross section for different systems induced by exotic, weakly, and strongly bound projectiles. The solid line is the result of a São Paulo potential calculation for the  ${}^6\text{Li}$  scattering on  ${}^9\text{Be}$  target. Dashed and dotted lines are a guide to the eyes.

3b-, and 4b-CDCC analysis [15] have been reduced using the relations below [20,21]:

$$\sigma_{\text{red}} = \frac{\sigma_{\text{exp}}}{(A_1^{1/3} + A_2^{1/3})^2}, \quad (2)$$

$$E_{\text{red}} = \frac{E_{\text{cm}}(A_1^{1/3} + A_2^{1/3})}{Z_1 Z_2}. \quad (3)$$

The goal of the reduction procedure is to allow the comparison among different systems at different energies in the same plot. This is done by rescaling the cross sections and energies, taking into account the size and the different Coulomb energies.

In Fig. 2 we compare the results for  ${}^6\text{He}$  and several other light projectiles on  ${}^9\text{Be}$  target [16,22–31]. The reduced values have been averaged over the different calculations (OM, CC, 3b-, and 4b-CDCC) and are plotted in Fig. 2 with an error bar given by the standard deviations of the four calculations included in the average (Table II). It is clear that systems involving the  ${}^6\text{He}$  nucleus present a much higher reduced reaction cross section compared to the stable double magic  ${}^4\text{He}$  nucleus. A surprising feature is the low-energy region ( $E_{\text{red}} < 1.0$ ) in Fig. 2, where most stable nuclei both weakly or tightly bound have very similar behavior. This was already observed for the  ${}^{12}\text{C}$  target in Ref. [13].

The question now lies in the comparison between the  ${}^6\text{He}$  and other weakly bound  ${}^{6,7,8}\text{Li}$  and  ${}^{7,9}\text{Be}$  projectiles. Is there any enhancement in the total reaction cross section or not and how it depends on the mass of the target? Albeit the dispersion in Fig. 2, there seems to be a sizable enhancement effect.

To investigate this point in more detail, the following quantity was calculated:

$$\Delta\sigma(\%) = 100 \frac{\sigma_{\text{reac}}({}^6\text{He}) - \sigma_{\text{reac}}({}^6\text{Li})}{\sigma_{\text{reac}}({}^6\text{Li})}, \quad (4)$$

where  $\sigma_{\text{reac}}({}^6\text{He})$  is the total reaction cross section induced by  ${}^6\text{He}$ , obtained from elastic scattering experiments for several

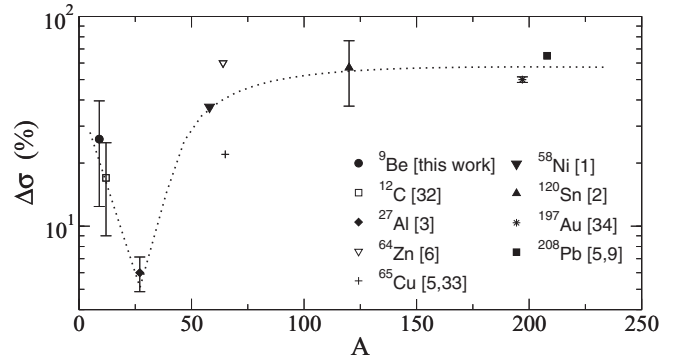


FIG. 3. Comparison between the enhancements [Eq. (4)] in the total reaction cross section for  ${}^6\text{He}$  and  ${}^6\text{Li}$  projectiles. The dashed line is a guide to the eyes.

systems [2,3,5,6,9,32–34]. Only experimental data taken at energies ( $E_{\text{red}} > 1.1$  MeV) were selected and the ratios have been calculated at the same reduced energies. This is an important point because, at energies below the Coulomb barrier, the cross sections drop down rapidly and it is difficult to quantify the differences between exotic and stable systems. For  $E_{\text{red}} > 1.1$  MeV, however, the differences among the systems seem to be less dependent on the energy and could be compared in a more reliable way. The quantity  $\sigma_{\text{reac}}({}^6\text{Li})$  was obtained from optical model calculations using the standard São Paulo potential (SPP) [35,36] and the results are shown in Fig. 2 by the solid line.

In Fig. 3 we plot  $\Delta\sigma(\%)$  as a function of the mass of the target. Considerable enhancements (60%) in the total reaction cross section are observed for  ${}^6\text{He}$  scattering on heavier targets such as  ${}^{120}\text{Sn}$  [2] and  ${}^{208}\text{Pb}$  [5,9]. This is expected from the effect of the Coulomb breakup, which is important for the scattering of neutron halo projectiles on heavy targets. For  ${}^6\text{He} + {}^9\text{Be}$ , on the other side, the situation is not so clear and smaller enhancements, of about  $\Delta\sigma = 22(7)\%$  for 16.2 MeV and  $31(18)\%$  for 21.3 MeV, are seen. The CDCC calculations applied to the  ${}^6\text{He} + {}^{12}\text{C}$  system [32] also show an enhancement of about 15% with respect to the weakly bound  ${}^6\text{Li}$ .

An interesting minimum in the enhancement is observed for the  ${}^6\text{He} + {}^{27}\text{Al}$  system [3] and the possible origin of this minimum requires further investigation.

The comparison of the reduced reaction cross sections between weakly bound and exotic projectiles as a function of the mass of the target is important because it allows one to display effects other than the pure geometrical ones. As explained before, enhancement effects in the total reaction cross section induced by exotic projectiles are probably related to their large breakup probabilities. The total breakup cross section is the result of the interference between two processes, Coulomb and nuclear breakups, and this interference can be either constructive or destructive, as shown in Ref. [10]. For heavy targets, both processes are important and interfere, but for light targets the nuclear breakup dominates. The interplay between Coulomb and nuclear breakup could then be assessed by an analysis of the enhancements as a function of the mass of the target.

In summary, we performed optical model fits of the  ${}^6\text{He} + {}^9\text{Be}$  scattering, separating the contribution of the fragment target and the dineutron target to the total projectile target interaction, and adjusting only the unknown dineutron target part. Very good fits of the angular distributions have been obtained and the resulting  $2n-{}^9\text{Be}$  potential presents a long-range diffuseness in the imaginary part.

A comparison among reduced reaction cross sections induced by several weakly bound stable projectiles  ${}^6,7,8\text{Li}$  and the exotic  ${}^6\text{He}$  on the light  ${}^9\text{Be}$  target indicate a possible

increase in the total reaction cross section for the  ${}^6\text{He}$  case, with respect to their weakly bound partners. This enhancement is of the order of twice the estimated error bars of the cross sections and was seen in the  ${}^6\text{He} + {}^9\text{Be}$  scattering at three energies and in the  ${}^6\text{He} + {}^{12}\text{C}$  system.

The authors acknowledge FAPESP (Fundação de Amparo à Pesquisa do Estado de São Paulo) and CNPq (Conselho Nacional de Desenvolvimento Científico e Tecnológico) for financial support.

- 
- [1] V. Morcelle *et al.*, *Phys. Lett. B* **732**, 228 (2014).  
 [2] P. N. de Faria *et al.*, *Phys. Rev. C* **81**, 044605 (2010).  
 [3] E. A. Benjamim *et al.*, *Phys. Lett. B* **647**, 30 (2007).  
 [4] M. Milin *et al.*, *Nucl. Phys. A* **730**, 285 (2004).  
 [5] E. F. Aguilera, I. Martel, A. M. Sanchez-Benítez, and L. Acosta, *Phys. Rev. C* **83**, 021601(R) (2011).  
 [6] A. Di Pietro *et al.*, *Phys. Rev. C* **69**, 044613 (2004).  
 [7] P. N. de Faria *et al.*, *Phys. Rev. C* **82**, 034602 (2010).  
 [8] I. Tanihata *et al.*, *Phys. Rev. Lett.* **55**, 2676 (1985).  
 [9] A. M. Sanchez-Benítez *et al.*, *Nucl. Phys. A* **803**, 30 (2008).  
 [10] M. S. Hussein, R. Lichtenthäler, F. M. Nunes, and I. J. Thompson, *Phys. Lett. B* **640**, 91 (2006).  
 [11] M. S. Hussein and R. Lichtenthäler, *Phys. Rev. C* **77**, 054609 (2008).  
 [12] T. Nakamura *et al.*, *Phys. Lett. B* **331**, 296 (1994).  
 [13] A. Barioni *et al.*, *Phys. Rev. C* **80**, 034617 (2009).  
 [14] J. C. Zamora *et al.*, *Phys. Rev. C* **84**, 034611 (2011).  
 [15] K. C. C. Pires *et al.*, *Phys. Rev. C* **83**, 064603 (2011).  
 [16] M. Majer, R. Raabe, M. Milin *et al.*, *Eur. Phys. J. A* **43**, 153 (2010).  
 [17] A. M. Moro, K. Rusek, J. M. Arias, J. Gomez-Camacho, and M. Rodríguez-Gallardo, *Phys. Rev. C* **75**, 064607 (2007).  
 [18] I. J. Thompson, *Comp. Phys. Rep* **7**, 167 (1988).  
 [19] C. M. Perey and F. G. Perey, *At. Data Nucl. Data Tables* **17**, 1 (1976).  
 [20] P. R. S. Gomes *et al.*, *Phys. Lett. B* **601**, 20 (2004).  
 [21] P. R. S. Gomes, J. Lubian, I. Padron, and R. M. Anjos, *Phys. Rev. C* **71**, 017601 (2005).  
 [22] R. B. Taylor, N. R. Fletcher, and R. H. Davis, *Nucl. Phys.* **65**, 318 (1965).  
 [23] F. P. Brady, J. A. Jungerman, and J. C. Young, *Nucl. Phys. A* **98**, 241 (1967).  
 [24] K. C. C. Pires, Ph.D. thesis, Universidade de São Paulo, 2011.  
 [25] P. L. Von Behren, E. Norbeck, and G. L. Payne, *Phys. Rev. C* **10**, 550 (1974).  
 [26] S. Verma *et al.*, *Eur. Phys. J. Special Topics* **150**, 75 (2007).  
 [27] F. D. Becchetti *et al.*, *Phys. Rev. C* **48**, 308 (1993).  
 [28] F. Lahlou, B. Cujec, and B. Dasmahapatra, *Nucl. Phys. A* **486**, 189 (1988).  
 [29] B. Dasmahapatra, B. Cujec, and F. Lahlou, *Nucl. Phys. A* **427**, 186 (1984).  
 [30] P. H. Barker, A. Huber, H. Knoth, U. Matter, A. Gobbi, and P. Marmier, *Nucl. Phys. A* **155**, 401 (1970).  
 [31] J. A. Kuehner and E. Almqvist, *Phys. Rev.* **134**, B1229 (1964).  
 [32] T. Matsumoto *et al.*, *Phys. Rev. C* **70**, 061601(R) (2004).  
 [33] A. Chatterjee *et al.*, *Phys. Rev. Lett.* **101**, 032701 (2008).  
 [34] K. Rusek, I. Martel, J. Gomez-Camacho, A. M. Moro, and R. Raabe, *Phys. Rev. C* **72**, 037603 (2005).  
 [35] L. C. Chamon *et al.*, *Phys. Rev. C* **66**, 014610 (2002).  
 [36] L. C. Chamon, D. Pereira, M. S. Hussein, M. A. Cândido Ribeiro, and D. Galetti, *Phys. Rev. Lett.* **79**, 5218 (1997).